Ann Microbiol (2017) 67:79–89
DOI 10.1007/s13213-016-1239-x

ORIGINAL ARTICLE

Genetic analysis of arsenic metabolism in *Micrococcus luteus* BPB1, isolated from the Bengal basin

Vrajan Vijay[1] · **Kozhikode Bhagavathiparambu Vandana**[1] · **Rajendran Mathan Kumar**[1] · **Solai Ramatchandirane Prabagaran**[1]

Received: 24 March 2016 / Accepted: 25 October 2016 / Published online: 29 November 2016

Abstract A highly arsenic-metabolizing bacterial strain was isolated from an agricultural field known for arsenic contamination near Munshiganj (Bangladesh). Based on 16S rRNA gene analysis, the strain was identified as *Micrococcus luteus* and designated as strain BPB1. Arsenate and arsenite minimal inhibitory concentrations of 650 mM and 7.5 mM, respectively, were observed for strain BPB1, slightly higher than the figures observed in its close relative *M. luteus* DSM 20030^T. Such observations were consistent with the presence of arsenic-metabolizing genes in the genome of *M. luteus*. We describe this strain as having an MSH/Mrx-dependent class of arsenate reductase, and an arsenite transporter family in the ACR3(1) group. Besides an intracellular arsenic resistance mechanism, experiments carried out using field emission scanning electron microscopy-energy dispersive X-ray spectroscopy (FESEM-EDS) and Fourier transform infrared spectroscopy (FTIR) demonstrated the ability of BPB1 to sequester arsenate in extracellular polymeric substances on its cell surface.

Keywords Arsenic · Soil bacteria · Arsenic resistance · Arsenate reductase · Arsenite transporter · Biosorption

✉ Solai Ramatchandirane Prabagaran
prabagaran@buc.edu.in

[1] Molecular Microbiology Laboratory, Department of Biotechnology, Bharathiar University, Coimbatore 641046, Tamil Nadu, India

Introduction

Arsenic (As) is a toxic metalloid, ubiquitously present in the environment with varied concentrations in different regions, causing serious health hazards. Arsenic contamination in natural resources is now a worldwide problem and often referred to as a calamity in the last century. Among the 21 countries in different parts of the world affected by groundwater arsenic contamination, the largest population at risk is in Bangladesh, followed by West Bengal in India (Lievremont et al. 2009). The adverse effects of As in groundwater used for irrigation to crops and aquatic ecosystems are a major threat to flora and fauna. Rice yield in Bangladesh has been reported to decrease by 10 % due to an As concentration of around 25 mg/kg in soil. Greenhouse studies have proven the reduction in yield of rice irrigated with water having As concentrations in the range of 0.2–8 mg/L (van Geen et al. 2006). The accumulation of As in field soils, and its introduction into the food chain through uptake by the rice plant is of major concern. Long-term exposure/ingestion of As causes skin, lung, bladder and kidney cancer as well as pigmentation changes, skin thickening (hyperkeratosis), neurological disorders, muscular weakness, loss of appetite and nausea (Bhattacharya et al. 2007; Mohan and Pittman 2007). Thus, As has been ranked first on the Superfund list of hazardous substances (Lin et al. 2006).

Arsenic toxicity depends on its speciation as it exists in several oxidation states (+5, +3, +2, +1 and −3), enabling it to mobilise under various environmental conditions. Among the As species, inorganic forms of As, i.e. pentavalent arsenate [As(V)] and trivalent arsenite [As(III)] are the most abundant in nature. Under oxidizing conditions, arsenate is the dominant form. However, the more toxic arsenite becomes dominant under reducing environments. In addition to abiotic transformation of arsenic, biotic processes, in which microorganisms play a key role, greatly influence arsenic

speciation. Under physiological conditions, arsenite binds to the sulphydryl groups of enzymes, and thus induces functional impairments. On the other hand, being a structural analogue of the phosphate ion, arsenate competes with it, causing many disturbances at the cellular level. It interferes in particular with the oxidative phosphorylation process, inhibiting the energy metabolism of cells (Lievremont et al. 2009; Tsai et al. 2009).

Arsenic contamination in soil provides an extreme environment for microbial growth. Indigenous microbes in nature tolerate high concentrations of heavy metals, and may play a vital role in restoring contaminated soils (Wei et al. 2009). Depending on their As resistance mechanism, microbes can influence the bioavailability of As compounds. Bacterial biotransformation of As through oxidation, reduction and methylation is a well-known phenomenon (Jia et al. 2013; Yang et al. 2012). One of the two known mechanisms of reduction is related to detoxification of cells, which is based on the expression of *ars* operon related genes, especially, arsenate reductase (ArsC) and a transmembrane efflux pump protein (ArsB /Acr3). Arsenate reductase reduces As(V) into the more toxic and soluble As(III), which is subsequently extruded out of cells via an arsenite transporter (Rosen 2002a, b; Tsai et al. 2009). In prokaryotes, based on the arsenate reduction mechanism, three distinct ArsC classes can be defined: (1) the glutathione (GSH)/glutaredoxin (Grx)-coupled class with only one thiolate nucleophile on the enzyme such as prokaryotic ArsC with a glutaredoxin-fold; (2) the thioredoxin (Trx)/ thioredoxin reductase (TrxR)-dependent class with the structural fold of low-molecular-weight protein tyrosine phosphatases (LMW-PTPase), and with the three thiolate nucleophiles on a single ArsC enzyme; and (3) the recently described mycothiol (MSH)/mycoredoxin (Mrx)-dependent class with the structural fold of LMW-PTPase, and with only one thiolate nucleophile on the ArsC enzyme (Villadangos et al. 2011). Similarly, two unrelated families of arsenite transporters have been described in bacteria: (1) the well-characterised ArsB permease, which has 12 transmembrane segments (TMs) and does not require thiol for As(III) and antimonite [Sb(III)] extrusion (Chen et al. 1996; Wu et al. 1992); and (2) the less known ACR3 family, which has nine or ten TMs and requires thiol for its arsenite transport mechanism (Fu et al. 2009; Wysocki et al. 2003). As one of its distant homologues from *Shewanella oneidensis* has shown to be selective for As(V) over As(III), substrate specificity for ACR3 is under debate (Xia et al. 2008; Yang et al. 2012). Phylogenetically, the ACR3 family can be further divided into two subgroups designated as ACR3(1) and ACR3(2) (Achour et al. 2007).

Several studies suggest that the reduction of arsenate to arsenite by microbes is involved in solubilisation of the element, resulting in the contamination of water sources (Lievremont et al. 2009). Thus, studying microbes with the capability to reduce arsenate can be of great impact because rice plants have been found to take up As(III) at a higher rate than As(V), which in turn affects public health to a higher degree (Bachate et al. 2009). In addition, since these bacteria play an important role in the geochemical cycling of arsenic, it seems reasonable to envisage using them in biosystems to treat As-contaminated sources (Chen et al. 2005; Srivastava and Majumder 2008; Vieira and Volesky 2000).

In this study, we report that an As-resistant strain of *Micrococcus luteus* was isolated from an As-contaminated agricultural field soil sample collected from Munshiganj (23° 5′ N 91° E), Bangladesh. The strain, designated BPB1, was further characterised because of its resistance to high levels of As. This is the first report supporting the hypothesis that the species may have MSH/Mrx-dependent class of arsenate reductase and ACR3(1) group of arsenite transporter family. We also demonstrate the ability of the strain to sequester arsenic on its cell surface.

Materials and Methods

Strain isolation and cultivation

Soil samples were collected from agricultural fields in Munshiganj (23° 5′ N 91° E) and Manikganj (23° 8′ N 89° 8′ E), Bangladesh. The soil sampling area is well documented as highly (100–1000 μg/L) As-contaminated regions in Bangladesh (Bhattacharya et al. 2009; Flanagan et al. 2012). Soil (1 g) was mixed in 9 mL sterile distilled water. All chemicals and reagents were procured from Himedia Laboratories, Mumbai, India. Serial dilutions were plated with 100 μL on nutrient agar (NA) medium (0.5 % peptone; 0.3 % beef extract; 0.5 % NaCl; 1.5 % agar; pH 7.1 ± 0.1) supplemented with 15 mM As(V) or 5 mM As(III). After 36 h incubation at 32 °C, based on colony morphology, different colonies were picked and streak-purified, and sub-cultured on Luria-Bertani (LB) agar medium supplemented with 15 mM As(V) (Achour et al. 2007). Minimal inhibitory concentration (MIC) of As for the isolates was determined by growing them in low phosphate medium (LPM) [80 mM NaCl; 20 mM KCl; 20 mM NH_4Cl; 3 mM $(NH_4)_2SO_4$; 1 mM $MgCl_2$; 0.1 mM $CaCl_2$; 2 μM $ZnSO_4$; 0.12 M Tris base; 0.5 % dextrose; 2 μg/mL thiamine; 1 % peptone; pH 7.1 ± 0.1] supplemented with various concentrations of arsenate (15–650 mM) and arsenite (5 mM, 7.5 mM and 10 mM) (Liu et al. 1995; Oden et al. 1994). MIC was defined as an increase in OD_{600} after 48 h of incubation at 32 °C; 100 μL of the 48-h culture was spread plated on NA medium. Viability was ascertained by their ability to grow on the NA medium within next 48 h. All reference strains and plasmid used in this study are given in Table 1. All grown cultures were stored at 4 °C for not more than 30 days.

Table 1 Reference bacterial strains and plasmids used in this study

Strains/plasmid	Genotype/description	Reference/source
Escherichia coli strains		
DH5α	*fhuA2Δ(argF-lacZ)U169 phoA glnV44 Φ80 Δ(lacZ)M15 gyrA96 recA1 relA1 endA1 thi-1 hsdR17*	New England Biolabs, Hitchin, UK
W3110	K12 F2 IN(*rrnD-rrnE*)	(Carlin et al. 1995)
WC3110	W3110*ΔarsC*::*kan*	(Mukhopadhyay et al. 2000)
AW3110	W3110*Δars*::*cam*	(Carlin et al. 1995)
Micrococcus luteus strain		
DSM 20030^T	Synonym of NCTC2665^T; Arsenic resistant *Actinobacteria;* Complete genome sequence accession number CP001628.1	DSMZ (Deutsche Sammlung von Mikroorganismen und Zellkulturen), Braunschweig, Germany
Plasmid		
pTZ57R/T	Amp^r lacZ, TA cloning vector	Fermentas, Waltham, MA

DNA extraction and PCR amplification

Genomic DNA was extracted from bacterial cultures by a modified method (Sambrook et al. 1989). The extracted DNA was visualised by ethidium-bromide-stained 0.7 % agarose gel electrophoresis (GeNei™, Bangalore, India) using UV gel documentation system (Alpha Digidoc Inc., USA). Plasmid was extracted from bacteria using plasmid purification kit according to the manufacturer's instructions (GeNei™, India).

Two sets of degenerate primers (Table 2) were designed to probe arsenite transporter [*ACR3(1)*] and arsenate reductase (*LMW-PTPase-ArsC*) in *M. luteus* isolates. A total of 10 *M. luteus* ACR3(1) and 100 bacterial LMW-PTPase-ArsC (WP_002855764) homologous protein sequences were obtained from NCBI-blast search. Conserved regions in each of the two protein families were identified using Block Maker and used to design consensus-degenerate hybrid oligonucleotide primers (CODEHOP) (Rose et al. 2003). The primer LMWP_F and LMWP_R was designed to amplify complete sequence of LMW-PTPase-ArsC gene from *M. luteus* DSM 20030^T. Purified genomic DNA from bacterial cultures was used as the template to optimise amplification conditions and to test the specificity of the degenerate primers. All PCR reaction mixtures contained approximately 50–100 ng DNA template, 1x PCR buffer, 1.5 mM $MgCl_2$, 0.2 mM deoxyribonucleoside triphosphates, 0.2 μM of each primer and 1U *Taq* DNA polymerase (Chromous Biotech, Bengaluru, India) in 25 μl volume. Amplifications were performed in a Master thermal cycler (Eppendorf, Germany). Cycling condition for all PCRs consisted of 5 min denaturation at 95 °C followed by 35 cycles of 1 min denaturation at 95 °C, 1 min annealing at 65–58 °C with a 1 °C decrement per cycle during the first 7 cycles and 1 min of primer extension at 72 °C. This was followed by a final extension reaction at 72 °C for 20 min. PCR products were purified with an agarose gel extraction kit (Qiagen, Valencia, CA) and stored at −20 °C.

Table 2 Primers used in this study for the amplification of 16S rRNA and arsenic (As) resistance-related genes

Primer name	Primer sequence (5′-3′)[a]	PCR product (bp)	Reference
fD1	GAGTTTGATCCTGGCTCAG	*16S rRNA* (1500)	Weisburg et al. 1991
rP2	ACGGCTACCTTGTTACGACTT		
darsC_F	ACSATYTAYCAYAAYCCG	*ArsC* (377)	Branco et al. 2008
darsC_R	TCGCCRTCYTCYTTSGWRAA		
LMWP_F	ATGACCACGAAGCGCCCTTC	*PTPase-ArsC* (430)	This study
LMWP_R	TCAGTTCGCGGTGCCGGT		
dLMWP_F	GCTGTTCGTGTGCGTGAARAAYGGNGG	*PTPase-ArsC* (357)	This study
dLMWP_R	CGATGTCGTCGCGCACNARNCKCAT		
ACR3(1)_F	GAAGGAGATGTCCTTCCTCG AYMGNTGGYT	*ACR3(1)* (964)	This study
ACR3(1)_R	GGACTTCGATCAGCGGNCCNACNAC		

[a] Degenerate nucleotide sites are indicated by standard ambiguity codes as follows: K = G or T; M = A or C; N = A, C, G or T; R = A or G; V = A, C or G; and Y = C or T

Cloning and sequencing

Purified PCR amplicons were ligated into a TA cloning vector pTZ5R/T as per the manufacturer's instructions (Fermentas InsTAclone™ PCR Cloning Kit, Fermentas, Waltham, MA). The products were used to transform chemically ($CaCl_2$) prepared competent cells of *Escherichia coli* DH5α (Sambrook et al. 1989). Plasmids from white colonies were screened for the presence of the correct size insert by restriction digestion using *Eco*RI (New England Biolabs, Hitchin , UK). Selected recombinant plasmids were sequenced by Scigenom Labs Pvt. Ltd. (Kochi, India).

Sequence analysis and phylogenetic tree

Post sequencing, the DNA sequences in the ABI chromatogram were edited and aligned manually with the help of Gene Runner version 3.05 (http://www.generunner.com) and Nucleotide BLAST (http://blast.ncbi.nlm.nih.gov/Blast.cgi). For bacterial identification, type strains having homology with the 16S rRNA gene sequence of the isolate was searched using the EzTaxon-e server (Kim et al. 2012); 22 sequences with the highest scores were then selected for evolutionary analysis. A type strain from each of the five different bacterial phyla was also included in the analysis (Achour et al. 2007). Evolutionary analysis was conducted using MEGA version 6 (Tamura et al. 2013). The neighbor-joining (NJ) distance method based on Kimura 2-parameter was used to construct phylogenetic tree, and the validity of the branches was ascertained with 1000 bootstrap replicates (Efron et al. 1996; Kimura 1980; Saitou and Nei 1987). For *arsC* and *ACR3* gene classification, sequences were compared to the entire GenBank nucleotide, amino acid and protein databases using BLAST programs (http://www.ncbi.nlm.nih.gov/Blast/). Phylogenetic analysis of deduced amino acid sequences were performed using MEGA version 5.1 (Tamura et al. 2011). The NJ distance method based on *p*-distance was used to construct phylogenetic trees, and the validity of the branches was ascertained with 1000 bootstrap replicates.

Characterisation of strain BPB1

In order to confirm sequestration of As by the strain BPB1, cells were harvested and then washed three times in 10 mL modified TAB solution (10 mM Tris base; 1 mM magnesium chloride; 150 mM potassium chloride; pH 7.1 ± 0.1) by centrifugation at 2500 *g* at room temperature and subsequently freeze-dried. The freeze-dried, arsenate-treated and untreated cells were analysed using field emission scanning electron microscopy-energy dispersive X-ray spectroscopy (FESEM-EDS) and Fourier transform infrared spectroscopy (FTIR). The freeze-dried samples were sprinkled lightly on carbon tape stickered on metal stubs and were coated with gold using sputter coater (Quorum Technologies, Q150RS, Laughton, UK). The gold-coated samples were viewed using FESEM (Quanta^{TM} FEG 250, FEI, Hillsboro, OR). The X-ray analyses were done using EDS (XFlash® Detector 5030, Bruker, Billerca, MA) operated at 20 kV coupled to the FESEM (Maldonado et al. 2010). Remnants of the same samples were used for FTIR spectroscopy (Giri et al. 2012; Villadangos et al. 2010). A Nicolet Avatar Model FT-IR spectrophotometer was used to record the IR spectra (4000–400 cm^{-1}) of the sample (5 mg) as KBr pellets.

Results and Discussion

Isolation and identification of As-resistant bacteria

Tolerance to As was defined as the ability to grow on NA plates containing either 15 mM As(V) or 5 mM As(III) at 32 °C. Forty-two As-tolerant bacteria with different levels of As tolerance were isolated from the two soil samples. For the isolate designated as BPB1 from the Munshiganj soil, growth was not inhibited at concentrations as high as 650 mM As(V) and 7.5 mM As(III) . Colonies of strain BPB1 grown on LB agar were creamy-yellow pigmented, convex, smooth, circular, and were observed as Gram-positive cocci. FESEM images of BPB1 indicated that the bacterium size is around 800 nm in diameter (Fig. 8a). The partial 16S rRNA sequence determined (1485 nt) was submitted to Genbank under accession number KF410697. Phylogenetic analysis for strain BPB1 formed a cluster comprising Actinobacteria, and it is most closely related to *M. luteus* (99.73 %) (Fig. 1).

As resistance genes in *M. luteus*

Given that strain BPB1 is phylogenetically related to *M. luteus* NCTC 2665^{T}, whose genome sequence has been completely sequenced (GenBank CP001628.1), it provides an insight into their putative As resistance related operon or genes (Young et al. 2010). Through in silico study of the strain NCTC 2665^{T} genome, it was found that the strain possesses an operon-like genetic cluster responsible for As resistance (Fig. 2). This includes two open reading frames (ORFs) annotated as trans-acting regulatory protein ArsR genes, one arsenite carrier ACR3 permease family related gene, one low molecular weight protein tyrosine phosphatases-arsenate reductase (LMW-PTPase-ArsC) family-related gene, and one oxidoreductase. As the deduced amino acid sequence analysis of two *ArsR* genes showed just 28 % (21/74) identity, they are designated as *arsR*1 and *arsR*2.

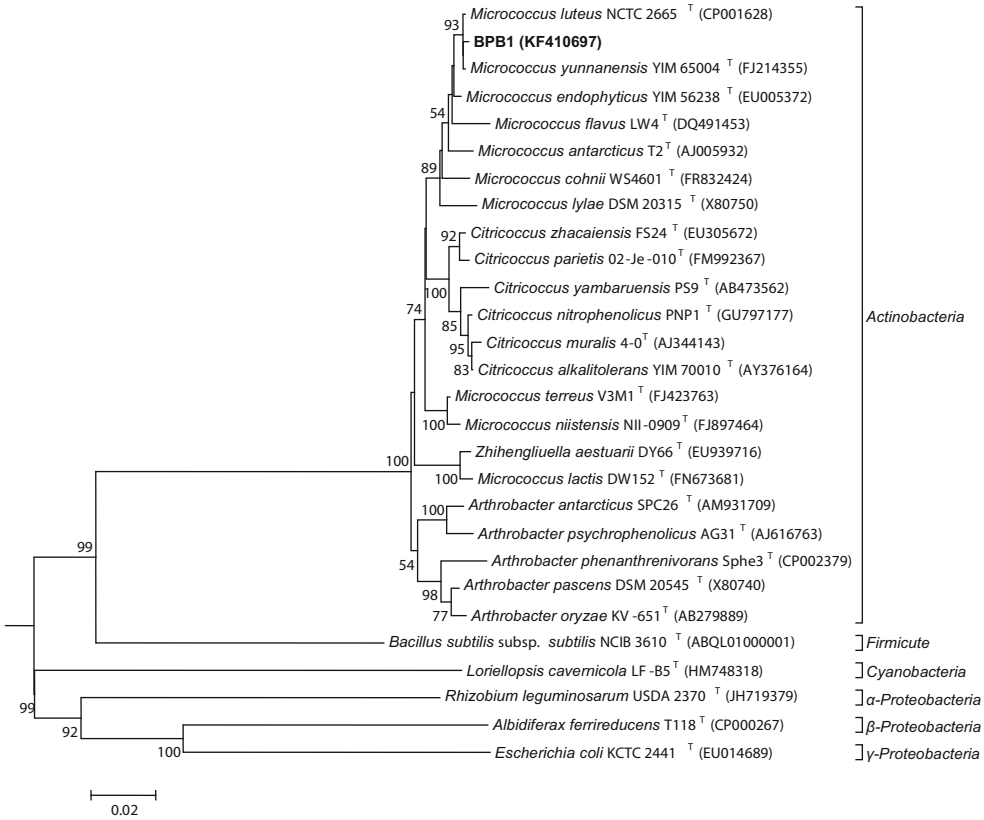

Fig. 1 Neighbour-joining tree based on 16S rRNA gene (1485 bp) sequence analysis. The GenBank accession numbers for the corresponding 16S rRNA gene sequences of type strains are given in parentheses. Bootstrap values (1000 replicates) over 50% are given at the nodes. Scale bar represents the number of substitutions per nucleotide position

Classification of arsenate reductase in *M. luteus*

Based on the gene sequence available from GenBank (GI:239916571), a set of gene-specific primers was designed for amplifying the *Ml_ArsC* gene in *M. luteus*. Genomic DNA from *M. luteus* DSM 20030^T and *E. coli* AW3110 (a mutant strain lacking the *ars* genes) were used as positive and negative controls, respectively (Carlin et al. 1995). In spite of successful amplification of the gene from DSM 20030^T, this primer could not amplify *Ml_ArsC* from isolate BPB1. This throws light on the diverse nature of the As-resistance-related genes within a single species. To this end, a set of degenerate primers targeting the partial sequence of *Ml_ArsC* was designed with the CODEHOP program. Subsequently, a 357-bp fragment of the putative *Ml_ArsC* from *M. luteus* strains DSM 20030^T and BPB1 was successfully amplified and sequenced. The nucleotide sequence identity between the partial *Ml-ArsC* gene sequences of *M. luteus* BPB1 and DSM20030^T was found to be 92 %. A phylogenetic tree of the translated amino acid sequences of *Ml-ArsC* genes was constructed with the previously known class of arsenate reductase (Fig. 3). Results placed the deduced ArsC amino acid sequences into three distinct clusters containing the well-characterised glutaredoxin-linked, thioredoxin-linked and mycoredoxin-linked ArsC proteins. It was also observed that the ArsC sequence of *M. luteus* was closely related to the previously known MSH/Mrx-dependent arsenate reductase proteins of *Corynebacterium glutamicum*.

Thus, the *Ml_ArsC* can be classified into the MSH/Mrx-dependent arsenate reductase family. ArsC of DSM 20030^T showed a higher sequence similarity with *C. glutamicum* ArsC1 (58 %) as compared to *C. glutamicum* ArsC2 (53 %). Similarly, while sequence identity of ArsC of BPB1 with that of DSM 20030^T was 95 %, it was 62 % and 54 % with Cg_ArsC1 and Cg_ArsC2, respectively. This confirms the highly diverse nature of this class of arsenate reductase

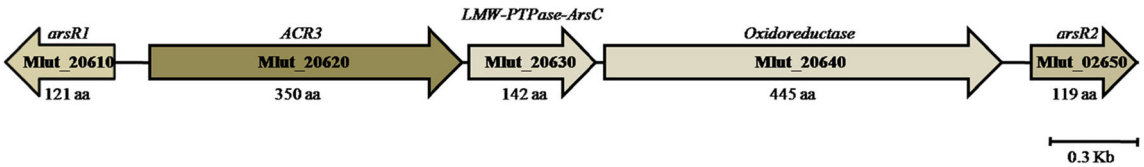

Fig. 2 Genetic organisation of arsenic (As) resistance related genes in the genome of *Micrococcus luteus* NCTC 2665^T. Putative As resistance related genes, locus_tag and protein product size are shown as shaded arrows. *arsR* is transcriptional regulator and *ACR3* is an arsenite transporter. *LMW-PTPase-ArsC* is low molecular weight protein tyrosine phosphatase related arsenate reductase. Note: The genome of *M. luteus* NCTC 2665^T also contains an oxidoreductase gene in the operon, whose role in As resistance is unknown

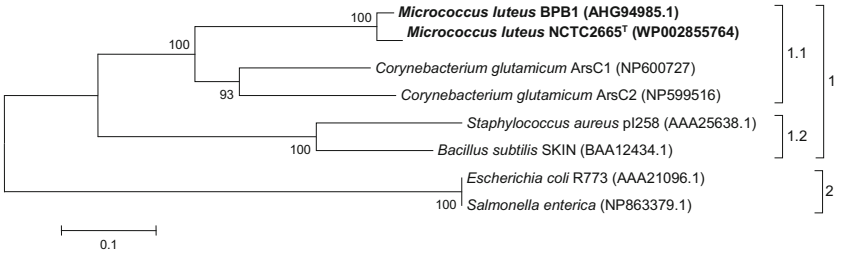

Fig. 3 Phylogenetic tree of inferred amino acid sequences of three different arsenate reductase (ArsC) classes. (1) Low molecular weight protein tyrosine phosphatases (LMW-PTPase) related ArsC; (1.1) Mycoredoxin-linked ArsC; (1.2) Thioredoxin-linked ArsC; and (2) Glutaredoxin-linked ArsC. *Numbers* at *nodes* represent bootstrap confidence values obtained with 1000 resamplings; values below 50 are not shown

proteins within bacterial species. From the multiple sequence alignment of amino acids of various classes of arsenate reductase, it was found that, despite the highly divergent amino acid sequence of Ml-ArsC, it has many conserved active site residues resembling MSH/Mrx-ArsC (Fig. 4). Ml_ArsC has a lone thiol nucleophile (C_N) at the N-terminal end of an α-helix. The protein tyrosine phosphatases loop (P-loop) signature motif (CX_5K) of Ml_ArsC is the same as that of MSH/Mrx-ArsC. The thiol group of the cysteine residue in the P-loop signature motif (CX_5R/K) is a catalytic site for all classes of PTPases, where an oxyanion arsenate binds. In Ml_ArsC, the positively charged lysine 64 (K64) of Cg_ArsC2 is replaced by polar glutamine (Q68). The charged amino group of K64 at the start of a hydrogen-bonding network decreases the pKa of the nucleophilic cysteine (C_N) thiol (Villadangos et al. 2011). In Ml_ArsC, the polar Q68 may take over the role of K64 as the start of a hydrogen-bonding network via polar N15 to C_N. As in MSH/Mrx-ArsC, the D106 and E107 of Ml_ArsC are located too far away from the nucleophilic cysteine to be functional as a general acid in dephosphorylation activity. Thus, like its homologue, the Ml_ArsC may not show phosphatase activity. The presence of these sequence characteristics in Ml_ArsC protein, typical of MSH/Mrx-ArsC, suggests that it can reduce arsenate by a mycothiol/mycoredoxin-dependent arsenate reductase mechanism (Villadangos et al. 2011). Owing to the high arsenate resistance of *M. luteus*, as well as very slow arsenate reductase activity of Mrx-ArsC of *C. glutamicum* (Ordonez et al. 2009), additional PCR amplification was carried out to search for other classes of arsenate reductase in *M. luteus* BPB1. For this purpose, a set of previously reported degenerate primers (P52F-P323R) was used (Branco et al. 2008). In spite of successful amplification of *ArsC* from *E. coli* W3110 DNA extract, there was no amplification in the case of *M. luteus*. This is in agreement with the in silico genome analysis result, where it was found that the *M. luteus* DSM 20030^T contains a lone *ArsC* gene in its genome. This result further confirms the absence of any other known class of arsenate reductase in *M. luteus*.

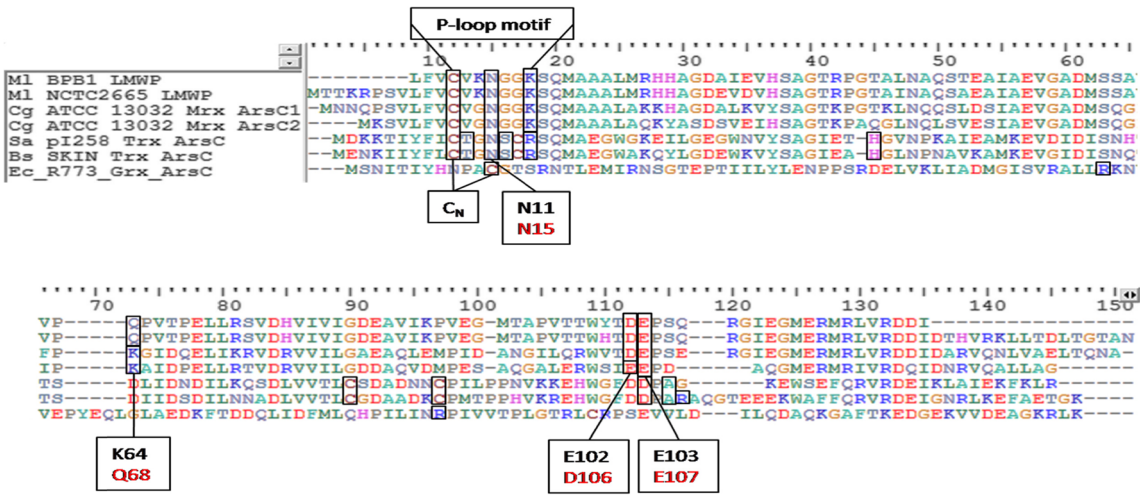

Fig. 4 CLUSTALW alignment of arsenate reductase proteins. Ml_LMWP_ArsC from *M. luteus* BPB1 (AHG94985.1) and DSM 20030 (GI:239918530) were aligned with two mycoredoxin linked arsenate reductase (Mer-ArsC) of *Corynebacterium glutamicum* [Cg_ArsC1 (GI:23308853) and Cg_ArsC2 (GI:19551514)], two thioredoxin linked arsenate reductase (Trx-ArsC) of *Staphylococcus aureus* plasmid pI258 (AAA25638.1) and *Bacillus subtilis* SKIN element (BAA12434.1), and one glutaredoxin-linked arsenate reductase of *Escherichia coli* plasmid R773 (AAA21096.1). P-loop motif refers to the LMW-PTPase signature CX5R motif. Catalytically important residues are shown in *boxes*. Residues indicated under the alignments are corresponding to Cg_ArsC2 (*black*) and Ml_ArsC (*red*)

Classification of arsenite transporter in *M. luteus*

The well-characterised ArsB permease can extrude both As(III) and antimonite [Sb(III)] (Chen et al. 1996; Wu et al. 1992). Since the *M. luteus* strains could not grow on LPM medium supplemented with 0.1 mM potassium antimonyl tartrate, their antimonite susceptibility confirmed lack of any active ArsB protein in them, whereas, Acr3 appeared to be more specific, transporting only arsenite but not antimonite (Sato and Kobayashi 1998; Wysocki et al. 1997), except in the case of *Synechocystis*, where the Acr3 was able to transport both arsenite and antimonite (Lopez-Maury et al. 2003). Hence, the substrate specificity for ACR3 is under debate (Xia et al. 2008; Yang et al. 2012). A set of degenerate primers was designed on the basis of the consensus sequence of *ACR3* genes retrieved from NCBI database by BLAST analysis of *ACR3* of *M. luteus* DSM 20030^T. Identity of the *ACR3* PCR product was confirmed by cloning and sequencing. There was 98 % nucleotide and 99 % amino acid sequence identity between the *ACR3* gene of isolate BPB1 and type strain DSM 20030^T. Phylogenetic analysis confirmed previous observations, i.e. arsenite transporters could be classified into two broad categories corresponding to the ArsB and ACR3 families (Wysocki et al. 2003), and the ACR3-like proteins could be further divided into two branches, which were designated as ACR3(1) and ACR3(2) subgroups (Achour et al. 2007). The phylogenetic analysis placed the deduced ACR3 amino acid sequences of *M. luteus* with the ACR3(1) of *C. glutamicum* (Fig. 5). Thus, the Ml_ACR3 can be classified into ACR3(1) group of ACR3 family of arsenite transporters. To predict transmembrane topology and active sites of the amino acid sequence from Ml_ACR3, its sequence was compared with previously characterised ACR3 proteins. Predictions for membrane topology of Ml_ACR3 from three different topological analysis programs, TopPred2, SOSUI, and TMHMM 2.0, generated two different theoretical models. TopPred2- and SOSUI-generated transmembrane models had nine TMs, with the N-termini localised in the cytosol and C-termini localised in periplasm, whereas, the Ml_ACR3 transmembrane model generated by TMHMM 2.0 had ten TMs, with the N- and C-termini localised in the cytosol (Fig. 6). Results obtained from TMHMM 2.0 were in concurrence with the membrane topology of ACR3(2) and ACR3(1) from *Alkaliphilus metalliredigens* and *Bacillus subtilis*, respectively (Aaltonen and Silow 2008; Fu et al. 2009). It is worth mentioning that, in all predicted models, the catalytically important and conserved residue Cys119 is located in the P/R-C-T/I-AMV motif of the fourth transmembrane region, whereas another important conserved residue Glu295 resides either in TM9 or in the cytoplasm-loop. Earlier studies done with ACR3 from *A. metalliredigens* [ACR3(2)] and *C. glutamicum* [ACR3(1)] had demonstrated the requirement of these residues for the arsenite transport mechanism (Fu et al. 2009; Yang et al. 2012). From the above observations, it is reasonable to speculate that Ml_ACR3 may have 10 TM spanning segments, with the – and C-termini localised in the cytosol, and both of the conserved residues (Cys119, Glu295) may serve as a selectivity filter for As (III).

Biosorption of arsenate by *M. luteus*

To confirm the sequestration of As(V) on the cell surface, cells from cultures treated with and without arsenate were subjected to FESEM coupled to EDS and FTIR analysis. The surface morphology of *M. luteus* BPB1 cells during the biosorption process was observed with the help of FESEM images (Fig. 7). *M. luteus* BPB1 bacteria without As(V) ion exposure in the control blank were cocci-like in shape and approximately 800 nm in diameter, and were aggregated to form irregular clusters (Fig. 7a). The formation of aggregates can be attributed to the secretion of extracellular polymeric substances (EPS) by these cells (Maldonado et al. 2010). EDS spectra of these cells confirmed the absence of As on their surface (Fig. 7b). After the As(V) ion exposure, no significant change in the morphology of cells were observed (Fig. 7c). The sorption of arsenate by these cells was determined by EDS

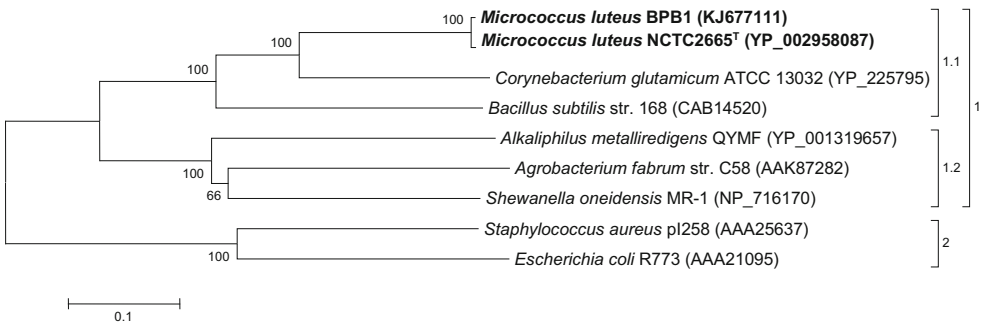

Fig. 5 Phylogenetic tree of inferred amino acid sequences of two different arsenite transporter families: *1* ACR3p; [1.1] ACR3(1)p; [1.2] ACR3(2)p; and *2* ArsB. Numbers at nodes represent bootstrap confidence values obtained with 1000 resamplings; values below 50 are not shown. The GenBank accession numbers for the corresponding arsenate reductase gene sequences are given in parentheses. *Bar* Substitutions per site

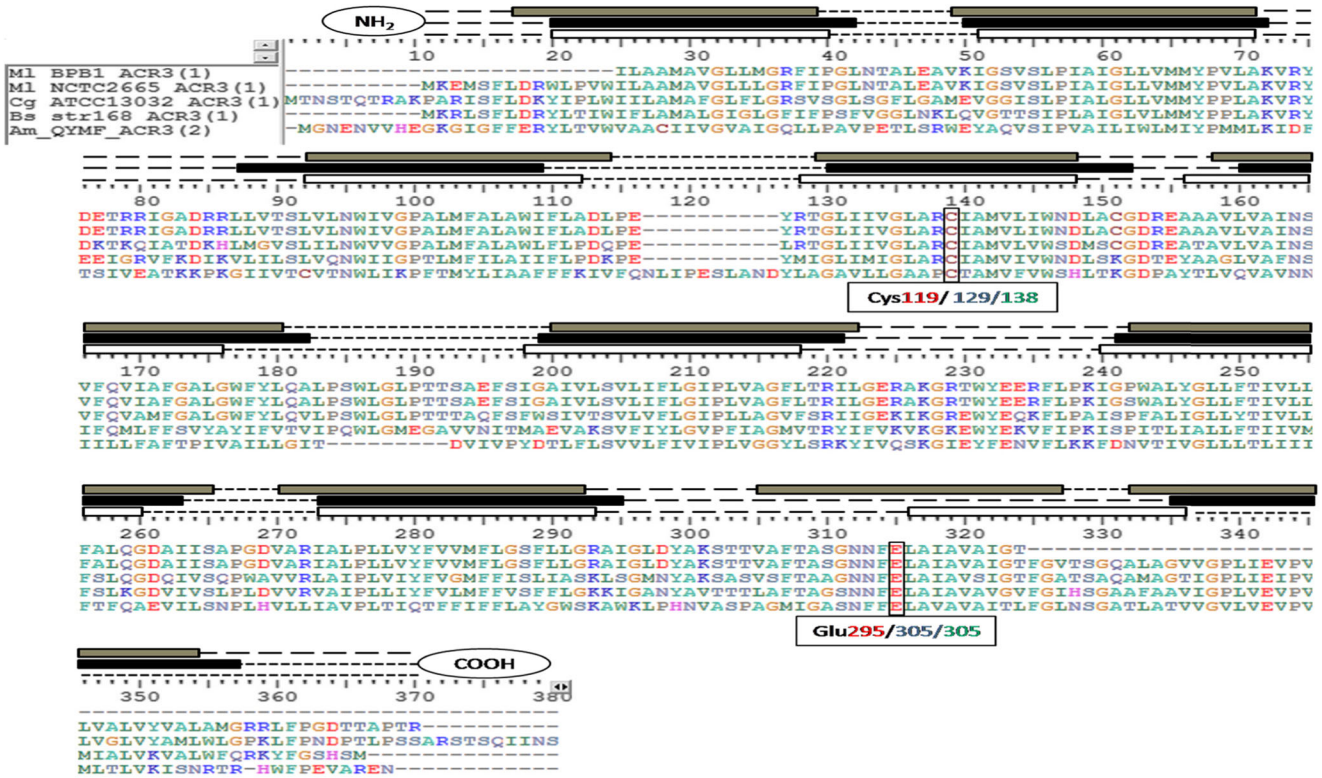

Fig. 6 CLUSTALW alignment of ACR3 proteins and predictions of the transmembrane topology of Ml_ACR3. Secondary structure predictions for Ml_ACR3 were generated from the primary amino acid sequence [Ml_NCTC2665_ACR3(1)] with TMHMM 2.0 (TMs in *shaded boxes*), SOSUI [transmembrane segments (TMs) in *filled boxes*], and TopPred2 (TMs in open boxes). TopPred2 and SOSUI predicted nine TMs, whereas TMHMM 2.0 predicted ten TMs. Each TM is connected with cytoplasmic (*long dashed lines*) and periplasmic loop (*dotted lines*). Residues indicated under the alignments are corresponding to Ml_ACR3(1) (*red*), Cg_ACR3(1) (*black*), Am_ACR3(2) (*green*). The conserved residue Cys119 is located in TM4 with all predictions

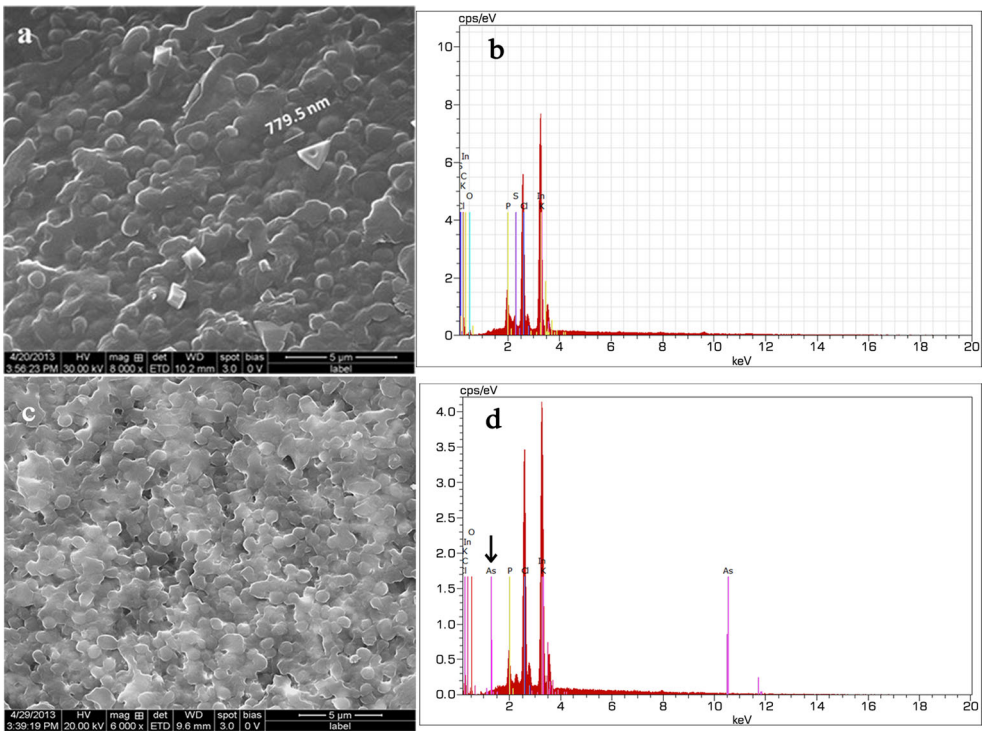

Fig. 7 FESEM image and EDS analysis spectra of *Micrococcus luteus* BPB1 culture: untreated (**a**, **b**) and treated (**c**, **d**) with 4 mM arsenate. EDS analysis spectra coupled to FESEM of arsenate treated cells has main arsenic (As) peak at 1.3 keV (arrow)

spectrum analysis. Two As peaks were obtained at 1.3 keV and 10.6 keV in the EDS spectrum of As(V) treated cells (Fig. 7d). The occurrence of multiple peaks for As can be attributed to the X-rays generated by emission from different energy-levels of K shell of the element (Abruzzi et al. 2013; Giri et al. 2013; Goldstein et al. 2012; Severin 2004). This result demonstrated that As was bound on the cell surface, probably with the functional groups of EPS. The FTIR spectra of BPB1 with and without arsenate-treated cultures were compared. The shifts in peaks at different wavelengths were analysed to determine the probable functional groups contributing to As ion sequestration (Fig. 8). The spectrum of the control biomass displayed a number of absorption peaks, indicating the complex nature of the bacterial biomass (Fig. 8a). The spectrum of control sample exhibited a broad absorption band at 3389.28 cm^{-1} due to the bonded –OH stretching vibration, which was shifted to 3357.46 cm^{-1} for arsenate-treated samples (Fig. 8b). This vibrational shift may have occurred due to the complexation of –OH groups with arsenate ions (Giri et al. 2013). There is no shift in the absorption peak for the amide group (N–H stretching and C = O stretching vibration) at 1653.66 cm^{-1} after As(V) exposure (Seki et al. 2005). The absorbance peaks at 1456.96 cm^{-1}, which may be attributed to N–H stretching vibration, $-CH_2$ scissoring or –

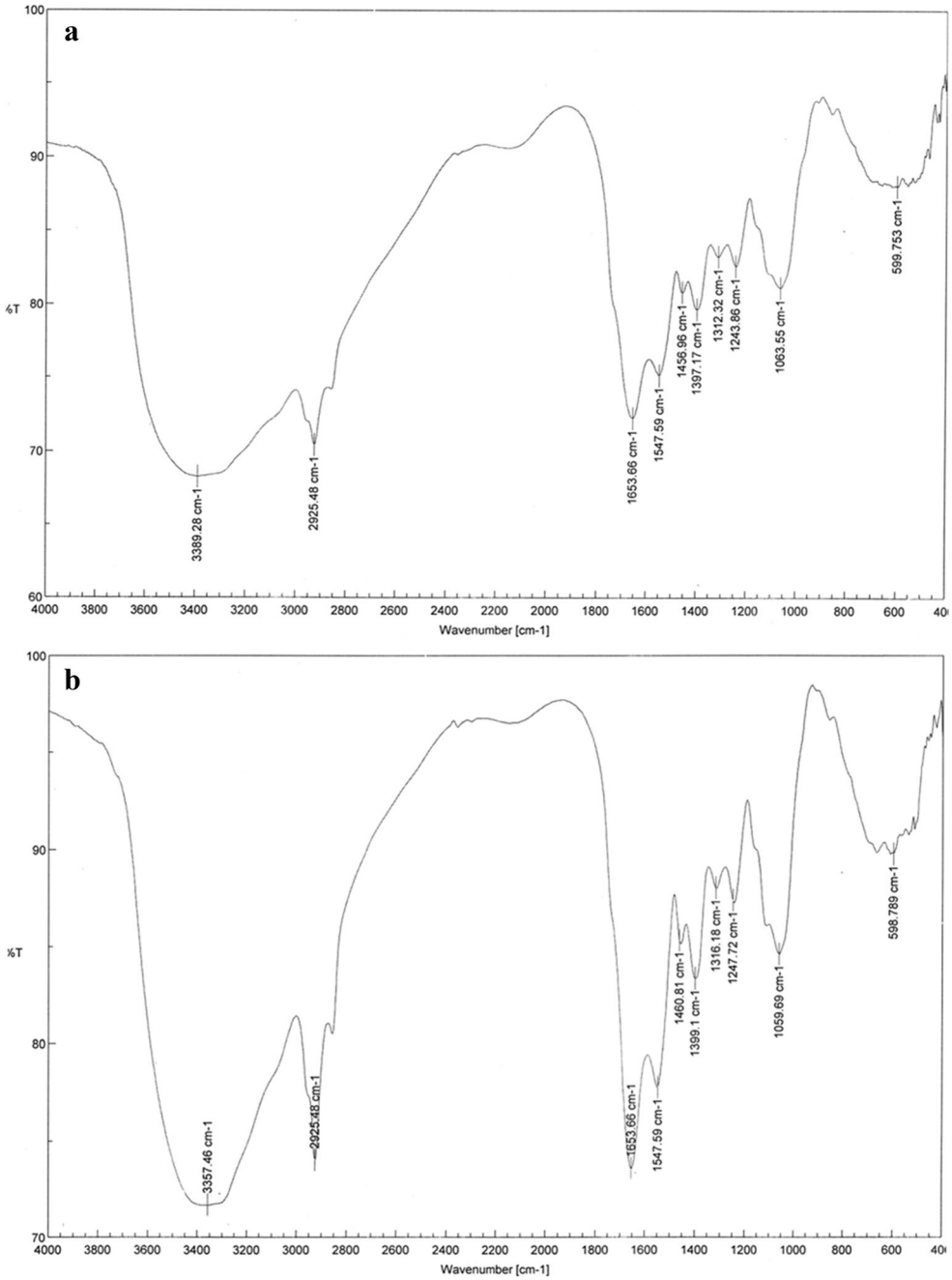

Fig. 8a,b Fourier transform infrared spectroscopy (FTIR) spectra of *M. luteus* BPB1 biomass. **a** Control, **b** arsenate treated

CH_3 antisymmetrical bending vibration and O–H deformation has shifted to higher frequency, and appears at 1460.81 cm^{-1}, which may be due to the complexation of As(V) ions with the functional groups. The peaks at 1063.55 cm^{-1}, which may result from C–N stretching vibrations of amino groups, are now shifted to lower frequency and appear at 1059.69 cm^{-1} due to the interaction of nitrogen from the amino group with arsenate (Giri et al. 2013). The aforementioned changes in the spectrum can be explained by the interaction of As(V) with the hydroxyl, amide and amino groups present on the surface of the *M. luteus* BPB1 biomass. These agree with the results of EDS spectra analysis. Earlier studies have reported several bacterial strains, especially *Micrococcus* sp., *Pseudomonas* sp. and *Bacillus* sp. surviving under abiotic stress by producing EPS (Giri et al. 2012, 2013; Maldonado et al. 2010; Raza and Faisal 2013; Sandhya et al. 2009) Micro-organisms that can form biofilm by secreting polymers are able to immobilise metal compounds via a passive sequestration process (Davies et al. 2007; Lievremont et al. 2009; Muller et al. 2007)]. Similarly, from this study, it was found that the cells of *M. luteus* BPB1 can sequester As(V) ions on their cell surface, which can be attributed to the interactions between metal ions and functional groups of extracellular polymeric substances on the cell surface. However, the inability of *M. luteus* to completely sequester As from the medium even after 36 h of treatment, and the existence of As-resistance-related genes might mean that, unlike lead and copper, As can get into the cytosol.

Concluding remarks

This study found that, irrespective of their distinct geographical location, *M. luteus* isolates BPB1 and DSM 20030^T both showed resistance to high concentrations of arsenate and have *ars* operon-related genes in their genome. The primers developed in this work proved to be specific to MSH/Mrx-ArsC and ACR3(1) of *M. luteus*, indicating that they could be useful to further explore the diversity of key arsenic resistance genes in a variety of bacteria. Extensive comparison of the amino acid sequence of arsenate reductase and arsenite transporter from *M. luteus* with their homologous proteins classified them as belonging to the recently described MSH/Mrx-dependent class of arsenate reductase and the inadequately characterised ACR3(1) group arsenite transporter family, respectively. Besides the intracellular arsenic resistance mechanism, *M. luteus* isolate BPB1 demonstrated the ability to sequester arsenate in EPS on its cell surface, which may slow down As uptake by cells.

Acknowledgements The authors acknowledge the Department of Biotechnology (Government of India, New Delhi) for grant vide BT/PR10897/GBD/27/117/2008. V.K.B. acknowledges the University Grants Commission for the award of Research Fellowship (20-12/2009(ii)EU-IV). The authors acknowledge Barry P. Rosen, FIU College of Medicine for providing *ars* mutant strains.

References

Aaltonen EK, Silow M (2008) Transmembrane topology of the Acr3 family arsenite transporter from *Bacillus subtilis*. Biochim Biophys Acta 1778:963–973. doi:10.1016/j.bbamem.2007.11.011

Abruzzi RC, Dedavid BA, Pires MJR, Ferrarini SF (2013) Relationship between density and anatomical structure of different species of Eucalyptus and identification of preservatives. Mater Res 16: 1428–1438

Achour AR, Bauda P, Billard P (2007) Diversity of arsenite transporter genes from arsenic-resistant soil bacteria. Res Microbiol 158:128–137. doi:10.1016/j.resmic.2006.11.006

Bachate SP, Cavalca L, Andreoni V (2009) Arsenic-resistant bacteria isolated from agricultural soils of Bangladesh and characterization of arsenate-reducing strains. J Appl Microbiol 107:145–156. doi:10.1111/j.1365-2672.2009.04188.x

Bhattacharya P et al (2009) Groundwater chemistry and arsenic mobilization in the Holocene flood plains in south-central Bangladesh. Environ Geochem Health 31(Suppl 1):23–43. doi:10.1007/s10653-008-9230-5

Bhattacharya P, Welch AH, Stollenwerk KG, McLaughlin MJ, Bundschuh J, Panaullah G (2007) Arsenic in the environment: biology and chemistry. Sci Total Environ 379:109–120. doi:10.1016/j.scitotenv.2007.02.037

Branco R, Chung AP, Morais PV (2008) Sequencing and expression of two arsenic resistance operons with different functions in the highly arsenic-resistant strain *Ochrobactrum tritici* SCII24T. BMC Microbiol 8:95. doi:10.1186/1471-2180-8-95

Carlin A, Shi W, Dey S, Rosen BP (1995) The ars operon of *Escherichia coli* confers arsenical and antimonial resistance. J Bacteriol 177: 981–986

Chen Y, Dey S, Rosen BP (1996) Soft metal thiol chemistry is not involved in the transport of arsenite by the Ars pump. J Bacteriol 178: 911–913

Chen Z, Zhu YG, Liu WJ, Meharg AA (2005) Direct evidence showing the effect of root surface iron plaque on arsenite and arsenate uptake into rice (*Oryza sativa*) roots. New Phytol 165:91–97. doi:10.1111/j.1469-8137.2004.01241.x

Davies JA et al (2007) The GacS sensor kinase controls phenotypic reversion of small colony variants isolated from biofilms of *Pseudomonas aeruginosa* PA14. FEMS Microbiol Ecol 59:32–46. doi:10.1111/j.1574-6941.2006.00196.x

Efron B, Halloran E, Holmes S (1996) Bootstrap confidence levels for phylogenetic trees. Proc Natl Acad Sci USA 93:13429–13434

Flanagan SV, Johnston RB, Zheng Y (2012) Arsenic in tube well water in Bangladesh: health and economic impacts and implications for arsenic mitigation. Bull World Health Organ 90:839–846. doi:10.2471/blt.11.101253

Fu HL et al (2009) Properties of arsenite efflux permeases (Acr3) from *Alkaliphilus metalliredigens* and *Corynebacterium glutamicum*. J Biol Chem 284:19887–19895. doi:10.1074/jbc.M109.011882

Giri AK, Patel RK, Mahapatra SS, Mishra PC (2013) Biosorption of arsenic (III) from aqueous solution by living cells of *Bacillus cereus*. Environ Sci Pollut Res Int 20:1281–1291. doi:10.1007/s11356-012-1249-6

Giri AK, Patel RK, Mishra PC (2012) Biosorption of As(V) from aqueous solutions by living cells of *Bacillus cereus*. Water Sci Technol 66: 1699–1707. doi:10.2166/wst.2012.332

Goldstein J et al (2012) Scanning electron microscopy and X-ray microanalysis: a text for biologists, materials scientists, and geologists. Springer, Berlin

Jia Y, Huang H, Zhong M, Wang F, Zhang L, Zhu Y (2013) Microbial arsenic methylation in soil and rice rhizosphere. Environ Sci Technol 47:3141–3148

Kim OS et al (2012) Introducing EzTaxon-e: a prokaryotic 16S rRNA gene sequence database with phylotypes that represent uncultured species. Int J Syst Evol Microbiol 62:716–721. doi:10.1099/ijs.0.038075-0

Kimura M (1980) A simple method for estimating evolutionary rates of base substitutions through comparative studies of nucleotide sequences. J Mol Evol 16:111–120

Lievremont D, Bertin PN, Lett MC (2009) Arsenic in contaminated waters: biogeochemical cycle, microbial metabolism and biotreatment processes. Biochimie 91:1229–1237. doi:10.1016/j.biochi.2009.06.016

Lin YF, Walmsley AR, Rosen BP (2006) An arsenic metallochaperone for an arsenic detoxification pump. Proc Natl Acad Sci USA 103:15617–15622. doi:10.1073/pnas.0603974103

Liu J, Gladysheva TB, Lee L, Rosen BP (1995) Identification of an essential cysteinyl residue in the ArsC arsenate reductase of plasmid R773. Biochemistry 34:13472–13476

Lopez-Maury L, Florencio FJ, Reyes JC (2003) Arsenic sensing and resistance system in the cyanobacterium *Synechocystis* sp. strain PCC 6803. J Bacteriol 185:5363–5371

Maldonado J et al (2010) Isolation and identification of a bacterium with high tolerance to lead and copper from a marine microbial mat in Spain. Ann Microbiol 60:113–120

Mohan D, Pittman CU Jr (2007) Arsenic removal from water/wastewater using adsorbents—a critical review. J Hazard Mater 142:1–53. doi:10.1016/j.jhazmat.2007.01.006

Mukhopadhyay R, Shi J, Rosen BP (2000) Purification andcharacterization of Acr2p, the*Saccharomyces cerevisiae*arsenate reductase.J Biol Chem275: 21149–21157

Muller D et al (2007) A tale of two oxidation states: bacterial colonization of arsenic-rich environments. PLoS Genet 3, e53. doi:10.1371/journal.pgen.0030053

Oden KL, Gladysheva TB, Rosen BP (1994) Arsenate reduction mediated by the plasmid-encoded ArsC protein is coupled to glutathione. Mol Microbiol 12:301–306

Ordonez E et al (2009) Arsenate reductase, mycothiol, and mycoredoxin concert thiol/disulfide exchange. J Biol Chem 284:15107–15116. doi:10.1074/jbc.M900877200

Raza FA, Faisal M (2013) Growth promotion of maize by desiccation tolerant '*Micrococcus luteus*'-chp37 isolated from Cholistan desert, Pakistan. Aust J Crop Sci 7:1693

Rose TM, Henikoff JG, Henikoff S (2003) CODEHOP (COnsensus-DEgenerate Hybrid Oligonucleotide Primer) PCR primer design. Nucleic Acids Res 31:3763–3766

Rosen BP (2002a) Biochemistry of arsenic detoxification. FEBS Lett 529:86–92

Rosen BP (2002b) Transport and detoxification systems for transition metals, heavy metals and metalloids in eukaryotic and prokaryotic microbes. Comp Biochem Physiol A Mol Integr Physiol 133:689–693

Saitou N, Nei M (1987) The neighbor-joining method: a new method for reconstructing phylogenetic trees. Mol Biol Evol 4:406–425

Sambrook J, Fritsch EF, Maniatis T (1989) Molecular cloning vol 2. Cold Spring Harbor Laboratory Press, Cold Spring Harbor, NY

Sandhya V, Ali SKZ, Grover M, Reddy G, Venkateswarlu B (2009) Alleviation of drought stress effects in sunflower seedlings by the exopolysaccharides producing *Pseudomonas putida* strain GAP-P45. Biol Fertil Soils 46:17–26. doi:10.1007/s00374-009-0401-z

Sato T, Kobayashi Y (1998) The ars operon in the skin element of *Bacillus subtilis* confers resistance to arsenate and arsenite. J Bacteriol 180:1655–1661

Seki H, Suzuki A, Maruyama H (2005) Biosorption of chromium(VI) and arsenic(V) onto methylated yeast biomass. J Colloid Interface Sci 281:261–266. doi:10.1016/j.jcis.2004.08.167

Severin KP (2004) Energy dispersive spectrometry of common rock forming minerals. Kluwer, Dordrecht

Srivastava NK, Majumder CB (2008) Novel biofiltration methods for the treatment of heavy metals from industrial wastewater. J Hazard Mater 151:1–8. doi:10.1016/j.jhazmat.2007.09.101

Tamura K, Peterson D, Peterson N, Stecher G, Nei M, Kumar S (2011) MEGA5: molecular evolutionary genetics analysis using maximum likelihood, evolutionary distance, and maximum parsimony methods. Mol Biol Evol 28:2731–2739. doi:10.1093/molbev/msr121

Tamura K, Stecher G, Peterson D, Filipski A, Kumar S (2013) MEGA6: molecular evolutionary genetics analysis version 6.0. Mol Biol Evol 30:2725–2729

Tsai SL, Singh S, Chen W (2009) Arsenic metabolism by microbes in nature and the impact on arsenic remediation. Curr Opin Biotechnol 20:659–667. doi:10.1016/j.copbio.2009.09.013

van Geen A et al (2006) Impact of irrigating rice paddies with groundwater containing arsenic in Bangladesh. Sci Total Environ 367:769–777. doi:10.1016/j.scitotenv.2006.01.030

Vieira RH, Volesky B (2000) Biosorption: a solution to pollution? Int Microbiol 3:17–24

Villadangos AF et al (2010) Retention of arsenate using genetically modified coryneform bacteria and determination of arsenic in solid samples by ICP-MS. Talanta 80:1421–1427. doi:10.1016/j.talanta.2009.09.046

Villadangos AF et al (2011) *Corynebacterium glutamicum* survives arsenic stress with arsenate reductases coupled to two distinct redox mechanisms. Mol Microbiol 82:998–1014. doi:10.1111/j.1365-2958.2011.07882.x

Wei G, Fan L, Zhu W, Fu Y, Yu J, Tang M (2009) Isolation and characterization of the heavy metal resistant bacteria CCNWRS33-2 isolated from root nodule of *Lespedeza cuneata* in gold mine tailings in China. J Hazard Mater 162:50–56. doi:10.1016/j.jhazmat.2008.05.040

Weisburg WG, Barns SM, Pelletier DA, Lane DJ (1991) 16S ribosomal DNA amplification for phylogenetic study. J Bacteriol 173:697–703

Wu J, Tisa LS, Rosen BP (1992) Membrane topology of the ArsB protein, the membrane subunit of an anion-translocating ATPase. J Biol Chem 267:12570–12576

Wysocki R, Bobrowicz P, Ulaszewski S (1997) The *Saccharomyces cerevisiae* ACR3 gene encodes a putative membrane protein involved in arsenite transport. J Biol Chem 272:30061–30066

Wysocki R, Clemens S, Augustyniak D, Golik P, Maciaszczyk E, Tamas MJ, Dziadkowiec D (2003) Metalloid tolerance based on phytochelatins is not functionally equivalent to the arsenite transporter Acr3p. Biochem Biophys Res Commun 304:293–300

Xia X et al (2008) Investigation of the structure and function of a *Shewanella oneidensis* arsenical-resistance family transporter. Mol Membr Biol 25:691–705. doi:10.1080/09687680802535930

Yang HC, Fu HL, Lin YF, Rosen BP (2012) Pathways of arsenic uptake and efflux. Curr Top Membr 69:325–358. doi:10.1016/b978-0-12-394390-3.00012-4

Young M et al (2010) Genome sequence of the Fleming strain of *Micrococcus luteus*, a simple free-living actinobacterium. J Bacteriol 192:841–860. doi:10.1128/jb.01254-09